Topological configuration and demonstration of communication and micro grid network architecture for wide-area precision agriculture based on renewable energy resources

Shunsuke Yoshihara
Graduate School of Science and Technology
Chitose Institute of Science and Technology
Chitose, Japan
m2240520@photon.chitose.ac.jp

Shun Mito
Faculty of Science and Technology
Chitose Institute of Science and Technology
Chitose, Japan
b2222230@photon.chitose.ac.jp

Naoto Yoshimoto
Faculty of Science and Technology
Chitose Institute of Science and Technology
Chitose, Japan
n-yoshi@photon.chitose.ac.jp

***Abstract*—To realize more efficient precision agriculture leveraging AI, robotics, and other advanced technologies, the development of high-speed communication networks and reliable power infrastructures is essential. This study proposes a novel infrastructure for smart agriculture that integrates a communication network utilizing both optical and wireless technologies with a power distribution network based on renewable energy sources. The communication network employs optical wireless communication systems and Power over Ethernet (PoE) technology to achieve flexible scalability and high reliability. On the other hand, the power network adopts a decentralized autonomous control system using direct current (DC), which is highly compatible with solar power generation and contributes to simplified voltage control. To evaluate the feasibility of the proposed system, we conducted simulation-based comparisons of network topologies to ensure effective area coverage. Furthermore, a field network was constructed, and its sustainable operation was confirmed, demonstrating the practicality of the proposed system.**

Keywords—Precision agriculture, Communication and grid network convergence, DC power distribution network, Renewable energy resource, Zero-carbon operation, Internet of Things (IoT), Power over Ethernet (PoE), Optical network

I. Introduction

Precision agriculture has been increasing attention in recent years as a means to improve agricultural productivity, optimize resource utilization, and reduce environmental impact[1],[2]. By leveraging advanced technologies such as sensors, data analytics, and automation, precision agriculture enables site-specific crop management that leads to higher efficiency and sustainability[3],[4],[5]. At the same time, the growing awareness of climate change and environmental concerns has highlighted the importance of utilizing renewable energy sources in agricultural operations[6],[7],[8]. Integrating environmentally friendly energy solutions, such as solar or wind power, into smart farming systems not only reduces greenhouse gas emissions but also supports the development of resilient and decentralized energy infrastructures[9],[10]. In this context, the convergence of communication networks and microgrid systems plays a critical role in realizing sustainable and scalable precision agriculture. However, the use of broadband networks such as video streaming is currently limited to areas within several tens of meters from the optical network terminals provided by telecommunications carriers, such as barns and greenhouses, where Wi-Fi technology is typically employed. In contrast, for open-field cultivation across large-scale farmlands, Low Power Wide Area (LPWA) communication technologies such as LoRaWAN are commonly used. Although these technologies offer low data rates, they enable wide-area coverage[11]. As shown in Figure 1, realizing an advanced form of smart agriculture over large-scale farmlands requires the development of a new type of network infrastructure.

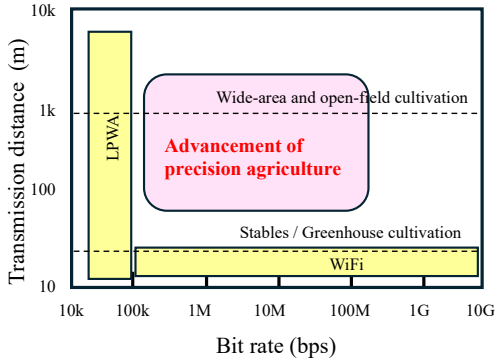

Fig. 1. Requirements for Communication Networks in Precision Agriculture

To achieve this goal, it is essential to effectively integrate broadband networks utilizing optical technologies with supporting power networks. In general, communication and power infrastructures are often underdeveloped in agricultural fields. Therefore, it is crucial to deploy these networks efficiently and ensure that they can

This work was partially supported by JST-OPERA (Open Innovation Platform with Enterprises, Research Institute and Academia), Japan Science and Technology Agency.

979-8-3315-6946-4/25/$31.00 ©2025 IEEE

be operated with simplicity and reliability[12],[13],[14]. We have previously proposed an integrated architecture that combines a communication network with a power network based on renewable energy sources to enable precision agriculture in agricultural fields as shown in Fig.2, and have evaluated its feasibility through experimental validation[15]. In this paper, we conduct a comparative study of network topologies within the previously proposed integrated architecture that combines communication and power networks to support precision agriculture, with the aim of effectively expanding network coverage. We also evaluate the technical feasibility and sustainability of the proposed system through field demonstrations. The remainder of this paper is organized as follows. Section 2 describes the configurations of the communication network and the power network, and then Section 3 presents a comparison of network topologies based on simulation results. Next, Section 4 discusses the field verification of the proposed system, and finally, overall conclusion of the paper is summarized in section 5.

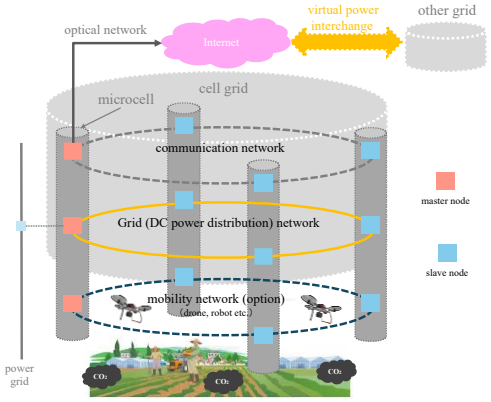

Fig. 2. Proposed concept of communication and grid network convergence for precision agriculture

II. NETWORK CONFIGURATION

This section describes the fundamental concepts of the communication network architecture and the power distribution network architecture. It also presents the structure of the micro cell, which serves as the fundamental building block for constructing these networks.

A. Communication network

First, Figure 2 shows the fundamental architecture of our network configuration. The communication network is divided into two segments: the section from the office, where the optical terminal provided by the telecommunications carrier is located, to the field, and the section within the field itself. The segment from the office to the master node (aggregating Layer 2 switch) in the field typically spans a long distance, but since it generally has a clear line of sight, free-space optical (FSO) communication is well-suited for this link. FSO communication offers a throughput of several hundred megabits per second, making it capable of transmitting various types of sensing data collected within the field. Within the field, the communication network is further divided into backbone routes and branch routes. The backbone routes, which connect communication nodes (Layer 2 switches), are established using optical fiber cables, offering high speed, long-distance scalability, and reliability. This setup is effective even in typical field environments where visibility may be obstructed by crops. The branch routes connecting communication nodes to various sensors are implemented using either wired Ethernet (IEEE 802.3ab: 1000BASE-T) or Wi-Fi (IEEE 802.11ac: Wi-Fi 5), depending on deployment requirements.

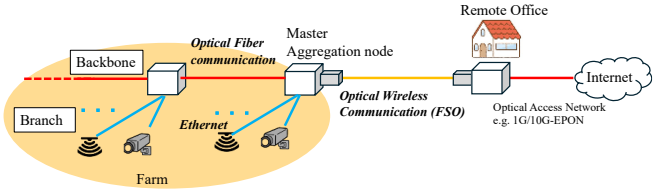

Fig. 3. Fundamental architecture of communication network

B. Power distribution netwok

Next, Figure 3 illustrates the fundamental architecture of the power network. Similar to the communication network, the power network within the field is divided into backbone routes and branch routes. The backbone routes, which connect power nodes (batteries), are configured in parallel using low-resistance electric cables that offer excellent scalability over long distances. The branch routes, which connect power loads such as communication nodes and various sensors to the batteries, utilize Power over Ethernet (PoE) technology, enabling both power and data transmission over Ethernet cables. Each unit cell consists of a battery, a solar panel, a charge controller, and a PoE node (PoE switch) as shown in Fig.5. These components are interconnected through the charge controller, which manages the connection between the battery, the solar panel, and the power-consuming devices including the PoE node.

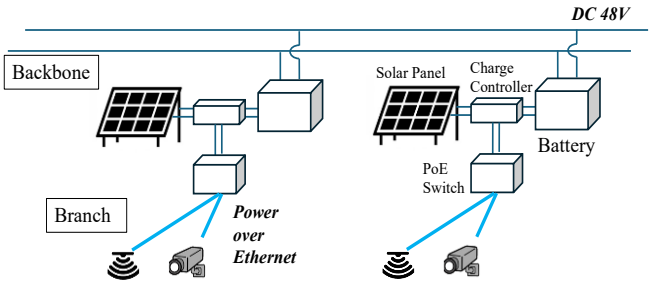

Fig. 4. Fundamental architecture of DC grid network and autonomous distributed cooperative coltage control model

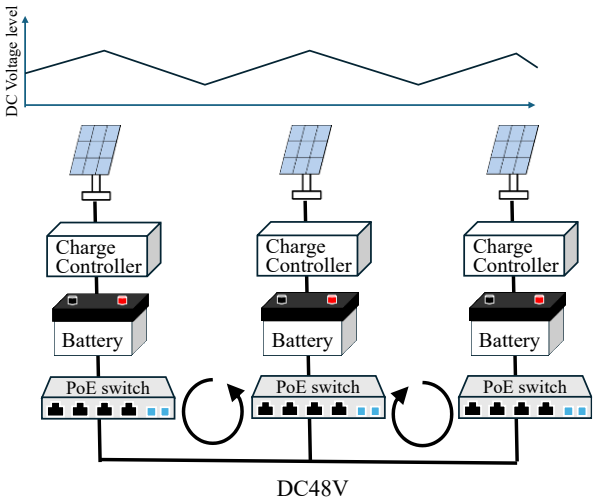

Fig. 5. Conceptual Diagram of Autonomous Distributed Cooperative Control of Power Network

The power source is based on renewable energy, specifically solar power generation. Therefore, power sharing within the network is carried out using a 48V DC system. When the power generation exceeds or matches the load consumption, the battery voltage in each unit cell remains nearly constant. Even when power generation is insufficient relative to the load, the battery voltages across connected cells autonomously reach an equilibrium state. This allows for seamless power supply from neighboring grids without requiring complex control systems, which is a key feature of the proposed architecture[16],[17],[18],[19]. Another feature of this configuration is that it allows for easy expansion of the power network area by connecting unit cells, without the need for complex voltage control functions. The voltage level of newly connected cells also autonomously transitions to a constant voltage[20].

III. Configuration and Interconnection of Cells

In order to efficiently cover a wide agricultural area, it is essential to examine the placement of cells that integrate the communication network nodes (Fig. 3) and the power network nodes (Fig. 4), along with their interconnection methods.

A. Relationship Between Cell Count and Inter-Cell Spacing

In this section, we begin by examining the appropriate number of cells for use in large-scale agricultural fields. First, we consider the number of cells based on the assumption that the agricultural field is a square with sides of 800 meters, resulting in a total area of 640,000 square meters. This area is approximately twice the average farmland size owned by farmers in Hokkaido, Japan, and can be considered sufficiently large. An example of cell placement within this area is shown in Fig. 6.

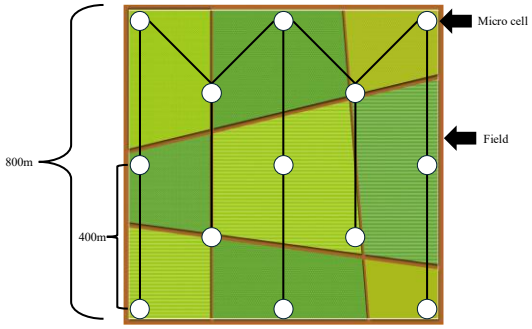

Fig. 6. Cell placement model

TABLE I. CELL COUNT AND INTER-CELL SPACING

N	Lmin [m]	Lmax[m]
5	564	800
9	400	564
13	282	400
25	200	282

Let the number of cells be denoted by N, the minimum distance between cells by L_{min}, and the maximum distance by L_{max}, as shown in Table 1. Assuming that the sensors connected to each cell are powered via PoE (Power over Ethernet) and can perform sensing within a 100-meter radius from each sensor, the maximum sensing coverage from a cell extends to a radius of 200 meters. Therefore, it is essential that L_{max}, does not exceed 400 meters, which implies that at least 13 cells are desirable. However, as the number of cells increases, both the number of cells themselves and the total length of connecting cables increase significantly, leading to a substantial rise in cost. Therefore, in this study, we proceed with the analysis assuming 13 cells, which meets the minimum spacing requirement while minimizing overall cost.

B. Cell Interconnection Method – Network Topology

The method of connecting cells is a critical factor that affects the overall reliability and cost of the grid. Therefore, in this study, we treated each cell as a node and examined the optimal connection method based on network topology. Among the various topologies commonly used in network design, we focused on the bus, ring, and tree topologies. Illustrative diagrams of these three configurations are shown in Fig. 7.

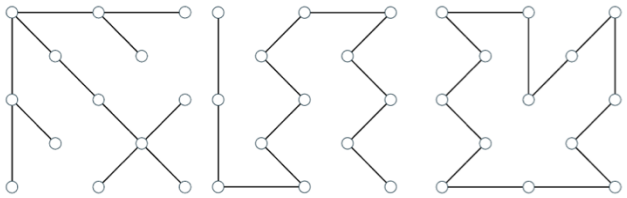

Fig. 7. Cell interconnection type: Tree (left) Bus (center) Ring (right)

First, regarding cost, the total cable length was 3,856 meters for both the bus and tree topologies, and 4,256 meters for the ring topology. However, since the tree topology requires more optical interfaces on communication nodes compared to the bus topology, it tends to be more expensive. Next, regarding scalability, we examined the number of extendable endpoints (cells) for each topology. In the bus topology, all cells must be connected along a single cable, so only the two endpoints can be extended. In the ring topology, adding a new cell requires rearranging the already connected cable to maintain the ring structure, resulting in zero easily extendable endpoints. In both cases, enhancing scalability would require adding more optical interfaces to the communication nodes within each cell. In contrast, the tree topology inherently includes communication nodes equipped with distribution-type optical interfaces, allowing expansion at any peripheral cell. Therefore, the number of extendable endpoints is 12. Finally, regarding maintainability, we consider two scenarios: damage to the solar panels and damage to the switching hubs or cables. In the event of solar panel failure, the bus and ring topologies can, in many cases, receive power from two adjacent batteries, enabling continued operation. However, in the tree topology, many cells are positioned at the periphery, and if a failure occurs in such a peripheral cell, it typically has only one adjacent battery. This results in a limitation in the available power supply, presenting a challenge for reliable operation. Next, in the case of failure in the switching hub or communication cables, both the bus and

tree topologies lose connectivity to all communication nodes located beyond the point of failure. In contrast, only the ring topology maintains connectivity regardless of which communication node fails, resulting in no impact on the surrounding system. The results of the comparison across the three topologies based on the evaluation criteria are summarized in Table 2. Based on the above analysis, the bus topology is considered the most advantageous when evaluating cost, scalability, and maintainability in total. Therefore, in this study, the bus topology was adopted for subsequent evaluations.

TABLE II. COMPARISON OF INTER-CELL CONNECTION TOPOLOGIES

Topology	Cost	Scalability	Maintainability
Bus	○	○	○
Tree	△	◎	△
Ring	△	△	◎

IV. AUTONOMOUS DISTRIBUTED COOPERATIVE CONTROL

The simulation verifies autonomous distributed cooperative control under a normal and a failure condition. The simulation was performed using MATLAB/Simulink. MATLAB/Simulink was used because it has a library of various electrical components, enabling the reproduction of various devices in the power network. The simulation was performed under the following conditions.

- The cell spacing was set to 400 m, and the resistance value was set to 1.4 Ω/km.
- Solar radiation data was obtained from Sapporo, Hokkaido, from April to September.
- The initial charge rate of the battery was set to 50%.
- The power consumption of the load was set to the same value as that of actual equipment.
- There were no obstructions in the vicinity, and the solar panels were able to generate sufficient power.

A. Normal condition

The simulation results of normal operation are shown in Fig.8. The results showed that autonomous distributed operation was performed without any problems. As shown in Fig., it was also found that even if the sensor load of some cells was large, the difference was not significant in the end. It was also confirmed that autonomous distributed operation was performed with the same results for all topologies.

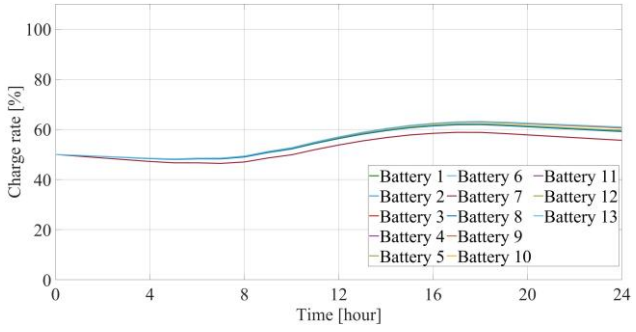

Fig. 8. Temporal Transition of Battery Charge Level under Normal Contidion

B. Failure condition

Figure 9 shows the results when solar panels are damaged in bus-type topology.

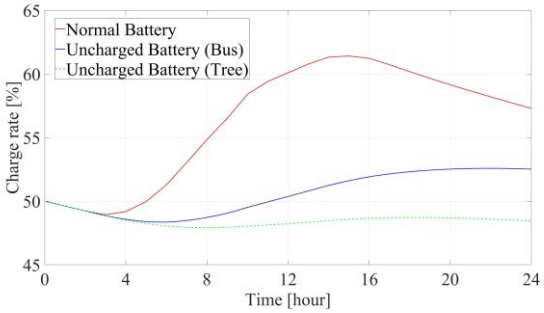

Fig. 9. Temporal Transition of Battery Charge Level under Failure Contidion

Although the bus type has a lower charge capacity than two adjacent batteries, its battery charge rate ultimately increases compared to the initial state, so it is considered that it can continue to operate without problems until recovery even if a failure occurs. In a tree-type topology, we confirmed that when there is only one adjacent battery, the charge rate falls below 50% of the initial charge rate, and the node itself may stop operating during operation. Therefore, it is considered that bus-type topology can operate stably even when a failure occurs, compared to tree-type topology.

V. EXPERIMENTS

The following section describes the results of deploying the microgrid in an experimental field on a university campus. An overview of the experimental field is shown in Fig. 10. The laboratory located on the university campus is connected via optical fiber cable to an optical wireless transceiver (Fraunhofer LIF-100) also installed on campus. From there, data is relayed to the experimental field using the optical wireless link, and within the field, cells are interconnected using optical fiber cables. This configuration enables high-capacity data transmission suitable for supporting precision agriculture.

Fig. 10. Aerial View of the Test Field

Fig. 11 shows the results of monitoring the optical wireless communication link. The optical transceiver utilizes 850 nm infrared light for data transmission, automatically performs beam alignment, and maintains a stable high-speed link by adapting the modulation scheme in response to fluctuations in received optical power caused by propagation conditions. As shown in the figure, a bidirectional throughput of over 400 Mbit per second has been achieved.

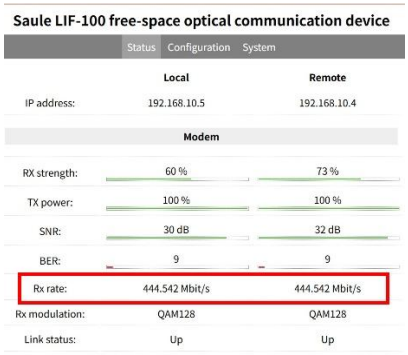

Fig. 11. Performance of optical wireless communicaiton

A. Experimetal Configuration

Figure 12 shows the microgrid in which three cells constructed within the experimental field are connected in a bus topology. The backbone cables between cells consist of composite cables (manufactured by OCC) that integrate low-resistance power lines and optical fibers, with a length of 100 meters. By using such shared cables, the overall cabling cost is reduced. Each communication node, consisting of a PoE switch installed in the cells, is equipped with two optical interfaces and transmits and receives data between nodes via SFP modules (1000BASE-LX). The power consumption of each PoE switch is approximately 7 W. By daisy-chaining these optical interfaces, additional cells can be easily connected through the composite cables, ensuring scalability. Simultaneously, the power lines within the composite cables allow batteries to be connected in parallel, enabling straightforward cell expansion from both power and communication perspectives.

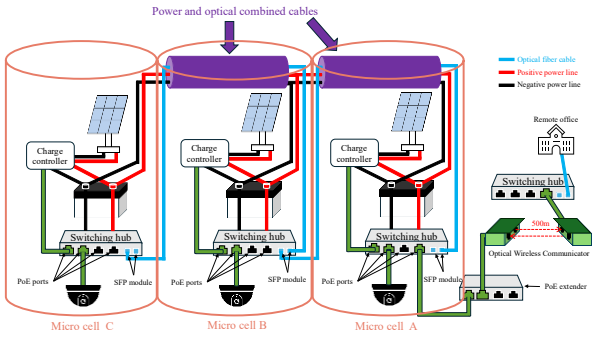

Fig. 12. System Configuration Diagram of the Field Experiment

Power is generated using solar panels (1.49 m × 0.66 m) with a nominal maximum output of 160 W. Serving as a power node, the TS-MPPT-60 charge controller (Morningstar Corp.) regulates the current from the solar panel to prevent battery overcharging and reverse current flow. The controller is connected to an IFM48-600E2 lithium-ion battery (DC 51.2 V), which stores the generated power. The charge controller is connected to the communication node via an Ethernet cable, allowing its status—including voltage levels—to be remotely monitored. On the other hand, the connections between the communication nodes and sensors, which form the branch lines, are established using PoE (Power over Ethernet) over Ethernet cables (100 meters in length). By enabling both data communication and power supply through a single cable, this approach reduces cabling costs and simplifies installation.

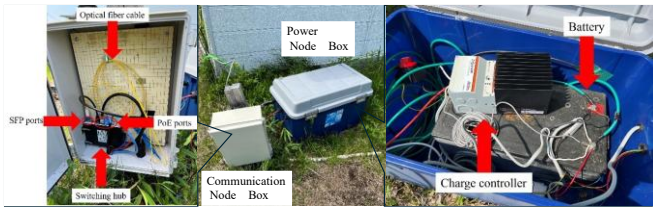

Fig. 13. Equipment Configuration within a Cell

B. Experimental Results

The simulation result of each battery state of charge conducted under the conditions described in Section 4 for the microgrid installed at the experimental site are shown in Fig. 14. All battery units operated without any issues during the summer farming season, and the microgrid as a whole functioned normally. The charge rate of Battery A is consistently higher than that of the other two batteries, which is attributed to its connection to a wireless optical communication device with a power consumption of 12 W.

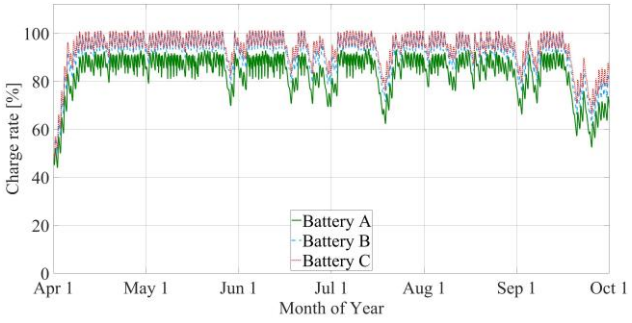

Fig. 14. Temporal Transition of Battery State of Charge accoding to the Configuration in Fig.12

Figure 15 shows an image captured by one of the surveillance cameras installed within the microgrid. As illustrated, grasslands and trees are clearly visible, indicating high image clarity. In this study, a total of three cameras, including the one shown in Fig. 15, were used. Each camera has a power consumption of approximately 6 W and all cameras successfully transmitted continuous video without any interruptions. These results confirm that the system can be effectively utilized for smart agriculture and similar applications, with sufficient optical communication capacity and no observed image distortion.

Fig. 15. Surveillance Camera Footage

Figure 16 presents the operational data collected from the actual microgrid. Battery A corresponds to the battery with microcell A (see Figure 12). Similarly, batteries B and C correspond to the batteries with microcells B and C, respectively. The data indicates that the voltages of all batteries remain well-coordinated. Since only Battery A is connected to a wireless communication device, its voltage tends to be the lowest among the three. However, it operates stably without any issues. While total power generation occasionally falls below consumption due to adverse weather conditions, it ultimately exceeds consumption overall. These results demonstrate that the microgrid functions reliably not only in simulations but also under real-world operating conditions.

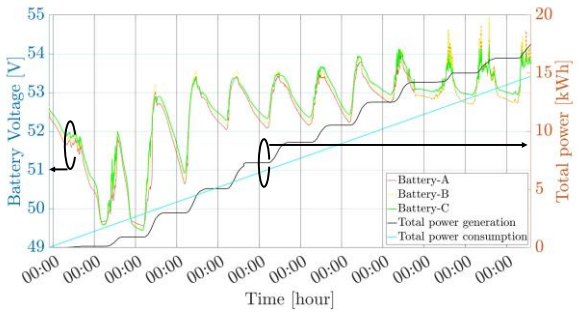

Fig. 16. Temporal Transitions of Each Battery's State of Charge, and Total Power Generation and Overall Power Consumption

VI. Summary

To support the promising future of precision agriculture, we have proposed a network that integrates communication and microgrids. In this study, assuming deployment across a wide agricultural field, we investigated the structure and interconnection methods of microcells, which are the components of the microgrid. We compared tree, bus, and ring topologies in terms of cost, scalability, and reliability. Among them, the bus topology demonstrated overall superiority, and we conducted simulations of the proposed microgrid based on this configuration to demonstrate its feasibility. Furthermore, based on the simulation results, we conducted a field experiment in a test farm. As a result, we confirmed that autonomous power sharing within the microgrid and sustainable transmission and reception of sensing data using only renewable energy were achieved, thereby demonstrating the effectiveness of the proposed approach.

Acknowledgment

This work was partially supported by JST-OPERA (Open Innovation Platform with Enterprises, Research Institute and Academia), Japan Science and Technology Agency. The authors would like to express their sincere gratitude to Prof. Taiichi Otsuji for his leadership and coordination of the research project. They also thank Dr. Katsumi Iwatsuki for his valuable support, and Prof. Hirohito Yamada for his insightful technical advice.

References

[1] M. Shepherd, J. A. Turner, B. Small, and D. Wheeler, "Priorities for science to overcome hurdles thwarting the full promise of the 'digital agriculture' revolution," *J. Sci. Food Agric.*, vol. 100, pp. 5083–5092, 2020, doi: 10.1002/jsfa.9346.

[2] Report Ocean Co. Ltd, "Report," 2022. [Online]. Available: https://newscast.jp/news/1235407

[3] G. Routis and I. Roussaki, "Low Power IoT Electronics in Precision Irrigation," Smart Agric. Technol., vol. 5, 100310, 2023, doi: 10.1016/j.atech.2023.100310.

[4] N. N. Thilakarathne, M. Saifullah, A. Bakar, M. A. Emeroylariffion, and H. Assin, "Internet of things enabled smart agriculture: Current status, latest advancements, challenges and countermeasures," Heliyon, vol. 11, e42136, 2025. [Online]. Available: www.cell.com/heliyon

[5] M. Aldossary, H. A. Alharbi, and C. A. Hassan, "Internet of Things (IoT)-Enabled Machine Learning Models for Efficient Monitoring of Smart Agriculture," IEEE Access, vol. 12, pp. 75718–75734, 2024.

[6] G. S. Malhi, M. Kaur, and P. Kaushik, "Impact of Climate Change on Agriculture and Its Mitigation Strategies: A Review," Sustainability, vol. 13, no. 3, 1318, 2021, doi: 10.3390/su13031318.

[7] S. Skendžić, M. Zovko, I. P. Živković, V. Lešić, and D. Lemić, "The Impact of Climate Change on Agricultural Insect Pests," Insects, vol. 12, no. 5, 440, 2021, doi: 10.3390/insects12050440.

[8] Japan Meteorological Agency, "Weather, Climate & Earthquake Information." [Online]. Available: https://www.jma.go.jp/jma/en/menu.html

[9] H. Ahmed and N. Shakoor, "Advancing agriculture through IoT, Big Data, and AI: A review of smart technologies enabling sustainability," Smart Agric. Technol., vol. 10, 100848, 2025, doi: 10.1016/j.atech.2025.100848.

[10] N. Abed, R. Murgun, A. Deldari, S. Sankarannair, and M. V. Ramesh, "IoT and AI-driven solutions for human-wildlife conflict: Advancing sustainable agriculture and biodiversity conservation," Smart Agric. Technol., vol. 10, 100829, 2025, doi: 10.1016/j.atech.2025.100829.

[11] A. Pagano, D. Croce, I. Tinnirello, and G. Vitale, "A Survey on LoRa for Smart Agriculture: Current Trends and Future Perspectives," IEEE Internet Things J., vol. 10, no. 4, pp. 3664–3679, Feb. 2023.

[12] A. Bathaei and D. Štreimikienė, "Renewable Energy and Sustainable Agriculture: Review of Indicators," Sustainability, vol. 15, no. 19, 14307, 2023, doi: 10.3390/su151914307.

[13] U. Daraz, Š. Bojnec, and Y. Khan, "Synergies between Sustainable Farming, Green Technology, and Energy Policy for Carbon-Free Development," Agriculture, vol. 14, 1078, 2024, doi: 10.3390/agriculture14071078.

[14] D. Avi1, A, T. Fayaz, B. B. Saha, and S. Ghosh, "Optimization of Solar, Wind and Biomass-Based Hybrid Renewable Energy System in St. Martin's Island, Bangladesh," in Proc. Int. Exchange Innov. Conf. Eng. Sci. (IEICES), vol. 7, pp. 122–128, 2021.

[15] S. Yoshihara, T. Maeda, D. Fukuda, and N. Yoshimoto, "Hybrid Configuration of Renewable Energy Sources for Carbon-Neutral Smart Sensing in Agricultural Field," in Proc. 23rd Chitose Int. Forum Sci. Technol. (CIF23), Chitose, Japan, Sep. 29–30, 2023, p. 17.

[16] T. Otsuji, K. Iwatsuki, H. Yamada, and M. Yashima, "Concept of Resilient Electric Power and Information Communication Technology (R-EICT) Converged Network Systems Based on Overall Optimization of Autonomous Decentralized Cooperative Control of DC Microgrids," in Proc. IEEE ISGT, 2021, paper 211SGT0018.

[17] K. Liu, H. Yamada, K. Iwatsuki, and T. Otsuji, "A study for stable operation of battery loaded DC bus based on autonomous cooperative control," in Proc. Int. Conf. Power Renew. Energy (ICPRE), 2021.

[18] K. Liu, Doctoral thesis, "Study on power sharing methods for autonomous decentralized coordinated control based DC microgrids," [Doctoral dissertation].

[19] Y. Nishita, K. Ishibashi, Y. Izui, H. Katayama, H. Yamada, and N. Yoshimoto, "Demonstration of wide-area electricity distribution using renewable energy by DC microgrid," Proc. ICEE Conf., to be submitted.

[20] S. Yoshihara, S. Oshima, R. Kamiya, R. Terada, and N. Yoshimoto, "Consideration of connected intra-grid power distribution methods for carbon neutrality," IEICE Tech. Rep., vol. 124, CS2024-15, pp. 29–32, 2024. [in Japanese]